

# Highly anisotropic decay rates of single quantum dots in photonic crystal membranes

Q. Wang,<sup>1,3</sup> S. Stobbe,<sup>1</sup> H. Thyrrestrup,<sup>1</sup> H. Hofmann,<sup>2</sup> M. Kamp,<sup>2</sup>  
T. W. Schlereth,<sup>2</sup> S. Höfling,<sup>2</sup> and P. Lodahl<sup>1,4</sup>

<sup>1</sup>*DTU Fotonik, Department of Photonics Engineering, Technical University of Denmark, Ørstedss Plads 343, 2800 Kgs. Lyngby, Denmark*

<sup>2</sup>*Technische Physik, Universität Würzburg, and Wilhelm Conrad Röntgen-Center for Complex Material Systems (RCCM), Am Hubland, D-97074 Würzburg, Germany*

<sup>3</sup>*E-mail: qinw@fotonik.dtu.dk*

<sup>4</sup>*E-mail: pelo@fotonik.dtu.dk*

Received April 15, 2010; revised June 9, 2010; accepted June 25, 2010;  
posted July 30, 2010 (Doc. ID 126135); published August 13, 2010

We have measured the variation of the spontaneous emission rate with polarization for self-assembled single quantum dots in two-dimensional photonic crystal membranes. We observe a maximum anisotropy factor of 6 between the decay rates of the two bright exciton states. This large anisotropy is attributed to the substantially different projected local density of optical states for differently oriented dipoles in the photonic crystal. © 2010 Optical Society of America

OCIS codes: 350.4238, 230.5298, 300.6470.

In the past few decades, there has been considerable interest in applying photonic crystals (PCs) for controlling the spontaneous emission (SE) of embedded emitters, which may find applications in diverse areas, such as quantum information science, efficient lasers, and LEDs. Originally proposed by Yablonovitch [1], the experimental progress has been delayed due to the lack of sufficiently high quantum efficiency emitters and PCs. The first experimental demonstrations of control of the spontaneous emission rate have appeared recently using colloidal quantum dots in three-dimensional opal PCs [2] and self-assembled quantum dots (QDs) or quantum wells in two-dimensional (2D) photonic crystal membranes (PCMs) [3–5] or PC cavities [6]. The latter technology has proven very successful due to the excellent optical properties of self-assembled QDs [7], the ability to optically address single QDs [4], and the strongly modified optical local density of states (LDOS) in PCMs [8]. Hitherto, plenty of research has been focused on the SE behavior of QDs embedded in PCs with defects [6,9,10] (e.g., a cavity or waveguide). PCs without defects have important merits, since they are less sensitive to spectral or spatial tuning of the QDs, thus providing a versatile method of controlling the SE rate of QDs. Recently it was theoretically proposed that the SE rate in a PC can be highly anisotropic depending on the orientation of the transition dipole moment of the emitter [11], which may be employed to enhance effects of quantum interference between the two radiating states [12] of relevance for quantum information applications. However, so far, no corresponding experimental demonstration has been reported to our knowledge. Here we experimentally demonstrate such a pronounced anisotropy by carrying out time- and polarization-resolved SE measurements on a single QD addressing two orthogonally polarized bright exciton states. In this process, we probe the anisotropy of the vacuum electromagnetic field in the PCMs, which was not addressed experimentally previously.

When optically exciting a QD, choosing the sample growth direction [001] as the quantization axis ( $z$ ) for

angular momentum, one lifts an electron ( $S_{e,z} = \pm \frac{1}{2}$ ) to the conduction band, leaving a heavy hole ( $J_{h,z} = \pm \frac{3}{2}$ ) in the valence band, which can form four possible exciton states ( $|h, e\rangle$ ):  $|\frac{3}{2}, -\frac{1}{2}\rangle$ ,  $|\frac{3}{2}, \frac{1}{2}\rangle$ ,  $|\frac{1}{2}, \frac{1}{2}\rangle$ ,  $|\frac{1}{2}, -\frac{1}{2}\rangle$ . We note that the light holes ( $J_{h,z} = \pm \frac{1}{2}$ ) can be neglected as the degeneracy of the light and heavy holes is lifted by the strain causing the QDs [13]. The four exciton states are categorized into two groups according to the values of their total angular momentum: bright states ( $J_z = \pm 1$ ) and dark states ( $J_z = \pm 2$ ), where only the bright states are optically active. Because of the reduced symmetry of self-assembled QDs and anisotropic exchange interactions, the two bright states are separated in energy (typically 0–30  $\mu\text{eV}$ ) and usually denoted as  $X$  or  $Y$  states according to their dipole orientations ( $[110]$  or  $[\bar{1}10]$ ). The photonic crystal patterns fabricated by electron-beam lithography can be aligned readily to these axes because they are normal to the natural cleave planes of standard (001) GaAs wafers. The QD SE decay curves are, in general, bi-exponential, where the fast component, which is considered here, is due to recombination of the bright exciton transitions, while the slow component is due to dark-state recombination mediated by spin-flip processes [14]. Polarization-resolved SE measurements enable addressing each of the orthogonally polarized bright exciton states individually and thereby allow us to probe the anisotropy of the vacuum electromagnetic field in the PCM. We quantify the polarization dependence by defining the anisotropy factor  $\eta^\gamma \equiv \frac{\gamma_X}{\gamma_Y}$ , where  $\gamma_X$  ( $\gamma_Y$ ) represents the decay rate of the  $X$  ( $Y$ ) states.

In our experiment, we used a standard micro-photoluminescence ( $\mu\text{PL}$ ) setup, see Fig. 1 of [9]. The sample is a GaAs PCM with a layer of self-assembled InAs QDs of density  $80 \mu\text{m}^{-2}$  embedded in the center of the membrane, as shown in Fig. 1(a). The excitation laser is a pulsed diode laser at 780 nm (1.59 eV) with a repetition rate of 20 MHz. To facilitate polarization-resolved measurements, a polarizer consisting of a half-wave plate

and a polarization beam splitter is used in the detection path. The excitation intensity used in the measurements is about  $300 \text{ mW/cm}^2$ , which is below the exciton saturation level, so that only photon emission from the ground state is observed. The ground-state emission energy is centered at  $1.36 \text{ eV}$  with an inhomogeneous broadening of  $140 \text{ meV}$ . The resolution of the monochromator is about  $120 \text{ } \mu\text{eV}$ , which is larger than the energy splitting between the two bright states. However, they can still be separated by their different polarizations.

In our experiments, we investigated about 30 different QDs positioned in seven different PCMs, with the lattice parameters ranging from  $260$  to  $325 \text{ nm}$ . For the sake of exploiting a pronounced 2D PC bandgap effect, we chose QDs in PCMs with  $r/a = 0.30$ , where  $r$  is the radius of the air holes and  $a$  is the lattice constant. For comparison, we also measured decay curves of four QDs positioned outside the PCMs. For each QD, the photoluminescence (PL) was projected onto different polarization directions by controlling the detection half-wave plate.

Figure 1(b) shows typical decay curves for two QDs, where QD A is inside a PCM, and QD B is in the unpatterned substrate while being close in emission energy to QD A. Three decay curves for QD A are displayed corresponding to different polarization components  $0^\circ$  (i.e., H),  $70^\circ$ , and  $90^\circ$  (i.e., V). We clearly observe that the SE rate is strongly dependent on polarization, illustrating that

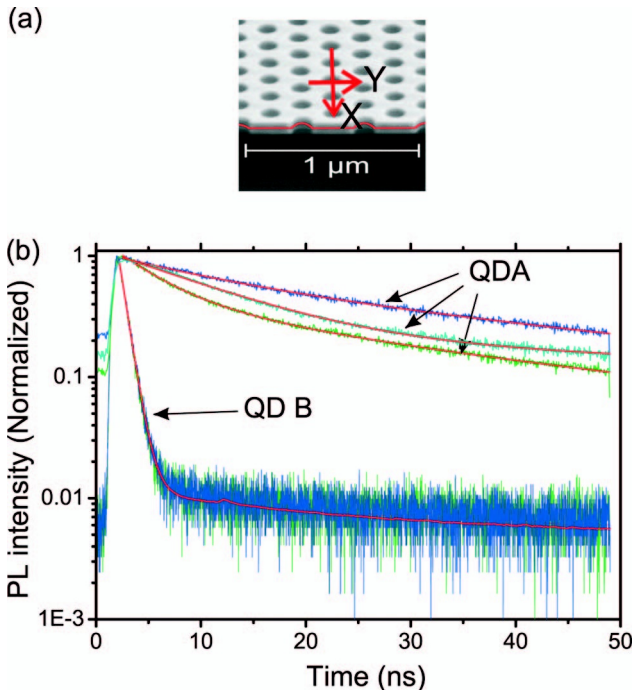


Fig. 1. (a) Scanning electron micrograph of the sample, in which a layer of self-assembled InAs QDs (red color) is embedded in the center of a GaAs PCM. The  $X$  and  $Y$  axes marked on the sample represent the  $X$  and  $Y$  dipole orientations ( $[110]$  or  $[\bar{1}10]$ ), respectively. (b) Three decay curves for QD A (inside PCM,  $a = 320 \text{ nm}$ , emission energy  $1.274 \text{ eV}$ ) corresponding to  $0^\circ$  (blue, upper curve),  $70^\circ$  (cyan, middle curve) or  $90^\circ$  (green, lower curve) polarization. Also shown are two decay curves for QD B (outside PCM, emission energy  $1.267 \text{ eV}$ ) for  $0^\circ$  (blue curve) and  $90^\circ$  (green curve) polarizations that are almost on top of each other. The red curves are bi-exponential fits to the decay curves.

$X$  and  $Y$  bright excitons decay significantly differently in the PCM due to the anisotropic vacuum fluctuations experienced by the QD. Note that the polarization-dependent decay rate reported here is fundamentally different from the anisotropic intensity distribution measured, e.g., for PC cavities in [15]. For comparison, no such anisotropy is observed in the reference measurements on QD B. The SE rate is found to be strongly inhibited in the PCM with inhibition factors differing for the  $X$  and  $Y$  states. By comparing QDs A and B, we derive an inhibition factor of  $15.8$  for the  $X$  state and  $6.5$  for the  $Y$  state.

The PL decay rate and intensity obtained when probing different polarizations for QD A are presented in Fig. 2. Polarizations H and V correspond to probing the two orthogonally polarized bright states  $X$  and  $Y$ , while intermediate directions probe a combination of the two bright states. Note that this implies that only in the former case are the decay curves strictly bi-exponential functions. However, this model turns out to model the decay curves rather well also for intermediate polarization settings, and the goodness-of-fit ( $\chi^2$ ) varying between  $1.0$  and  $1.4$  is found for the complete dataset. The PL intensity shows a maximum (minimum) value at H (V) polarization, which is opposite to the decay rate. This is expected since a stronger inhibition of the decay rate caused by the 2D photonic bandgap (PBG) means that less light propagates in the plane of the PCM, i.e., the emission efficiency in the direction normal to the PCM will be higher due to energy redistribution [3]. The PL intensity variation with polarization  $\theta$  is observed to follow the simple relation  $I = \frac{I_X + I_Y}{2} + \frac{I_X - I_Y}{2} \cos(2\theta)$ , where  $I_X$  and  $I_Y$  are the intensities of the  $X$  and  $Y$  exciton states, respectively; see Fig. 2. This can be easily understood as the result of applying polarization projection measurements on two orthogonal states.

Figure 3 shows the anisotropy factor of decay rates for all the measured QDs measured on PCMs with various values of the lattice constant. Note that all measurements presented are for QDs emitting within the 2D PBG of the PCMs [8], and all the QDs have fixed orientations of the transition dipole moment along the directions  $X$  and  $Y$ . The orientations of these dipole moments in relation to

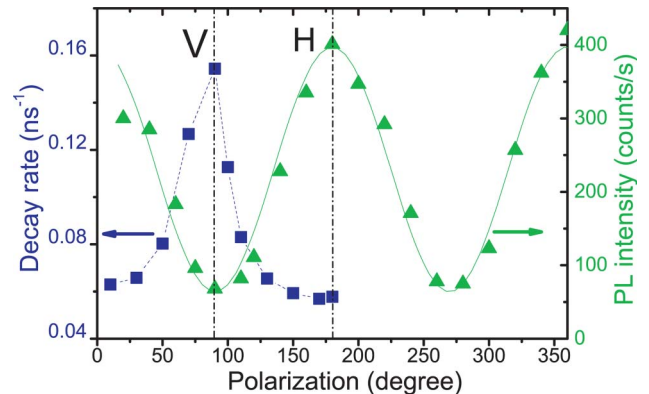


Fig. 2. (Color online) PL decay rates and intensities versus polarization for QD A. The square points (triangular points) are experimental results for decay rates (intensities). The solid curve is the fitted result with a cosine function, and the dashed curve is a guide to the eye.

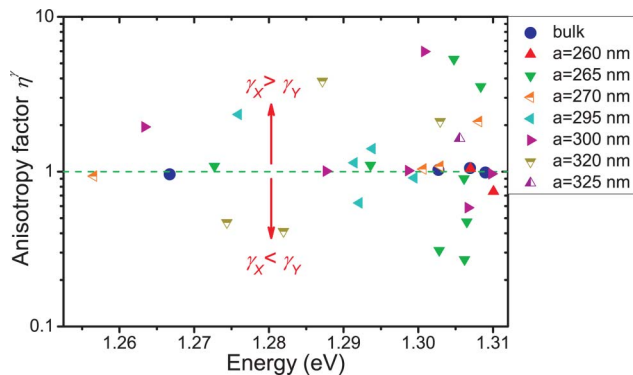


Fig. 3. (Color online) Measured anisotropy factor of decay rates between  $X$  and  $Y$  states. The triangular points represent QDs inside PCMs (with seven different lattice parameters); the circular points represent QDs outside PCMs, and the dashed horizontal line separates regions  $\gamma_X > \gamma_Y$  and  $\gamma_X < \gamma_Y$ .

the photonic crystal pattern have been indicated in the inset of Fig. 1(a). In the experiment, recording either an H or a V polarized photon corresponds to selecting light from an exciton with an  $X$  or a  $Y$  oriented transition dipole moment, respectively. As a result, the maximum and minimum value of decay rates locate either at H or V polarizations. Large variations are observed between the individual QDs in the PCM with a maximum value of about 6. This directly demonstrates the large anisotropy of the vacuum electromagnetic field in a PC that was theoretically proposed in [11]. This anisotropy gives rise to substantial differences in the projected LDOS, leading to the different decay dynamics of  $X$  and  $Y$  exciton states. For comparison, reference QDs in a bulk substrate showed no anisotropy in the decay rates for the two orthogonally polarized states.

To conclude, we have systematically measured the polarization-dependent SE rate for self-assembled single QDs inside PCMs and obtained a maximum anisotropy factor of decay rate between the  $X$  and  $Y$  states of 6. Our measurement results demonstrate the large anisotropy of the vacuum electromagnetic field inside PCMs [8,11], which is a crucial condition for achieving quantum interference between two closely lying energy levels [12] that could enable demonstration of fascinating phenom-

ena, such as lasing without inversion or quantum beats. Therefore, our experiment is not only vital in realizing complete control on the SE of single QDs with PCs, but also enables fundamental quantum optics experiments with practical systems.

We thank T. Lund-Hansen and M. L. Andersen for help during the experiment and gratefully acknowledge financial support from the Danish Research Council.

## References

1. E. Yablonovitch, Phys. Rev. Lett. **58**, 2059 (1987).
2. P. Lodahl, A. F. van Driel, I. S. Nikolaev, A. Irmann, K. Overgaag, D. Vanmaekelbergh, and W. L. Vos, Nature **430**, 654 (2004).
3. M. Fujita, S. Takahashi, Y. Tanaka, T. Asano, and S. Noda, Science **308**, 1296 (2005).
4. M. Kaniber, A. Laucht, T. Hürlimann, M. Bichler, R. Meyer, M. C. Amann, and J. J. Finley, Phys. Rev. B **77**, 073312 (2008).
5. B. Julsgaard, J. Johansen, S. Stobbe, T. Stolberg-Rohr, T. Sunner, M. Kamp, A. Forchel, and P. Lodahl, Appl. Phys. Lett. **93**, 094102 (2008).
6. A. Kress, F. Hofbauer, N. Reinelt, M. Kaniber, H. J. Krenner, R. Meyer, G. Böhm, and J. J. Finley, Phys. Rev. B **71**, 241304 (R) (2005).
7. J. Johansen, S. Stobbe, I. S. Nikolaev, T. Lund-Hansen, P. T. Kristensen, J. M. Hvam, W. L. Vos, and P. Lodahl, Phys. Rev. B **77**, 073303 (2008).
8. A. F. Koenderink, M. Kafesaki, C. M. Soukoulis, and V. Sandoghdar, J. Opt. Soc. Am. B **23**, 1196 (2006).
9. T. Lund-Hansen, S. Stobbe, B. Julsgaard, H. Thyrrerstrup, T. Sünner, M. Kamp, A. Forchel, and P. Lodahl, Phys. Rev. Lett. **101**, 113903 (2008).
10. G. Lecamp, P. Lalanne, and J. P. Hugonin, Phys. Rev. Lett. **99**, 023902 (2007).
11. W. L. Vos, A. F. Koenderink, and I. S. Nikolaev, Phys. Rev. A **80**, 053802 (2009).
12. G. S. Agarwal, Phys. Rev. Lett. **84**, 5500 (2000).
13. M. Bayer, G. Ortner, O. Stern, A. Kuther, A. A. Gorbunov, and A. Forchel, Phys. Rev. B **65**, 195315 (2002).
14. J. Johansen, B. Julsgaard, S. Stobbe, J. M. Hvam, and P. Lodahl, Phys. Rev. B **81**, 081304(R) (2010).
15. R. Oulton, B. D. Jones, S. Lam, A. R. A. Chalcraft, D. Szymanski, D. O'Brien, T. F. Krauss, D. Sanvitto, A. M. Fox, D. M. Whittaker, M. Hopkinson, and M. S. Skolnick, Opt. Express **15**, 17221 (2007).